

Measurement of CP Violation Parameters with a Dalitz Plot Analysis of $B^\pm \rightarrow D\pi^+\pi^-\pi^0 K^\pm$

B. Aubert,¹ M. Bona,¹ D. Boutigny,¹ Y. Karyotakis,¹ J. P. Lees,¹ V. Poireau,¹ X. Prudent,¹ V. Tisserand,¹
A. Zghiche,¹ E. Grauges,² L. Lopez,³ A. Palano,³ J. C. Chen,⁴ N. D. Qi,⁴ G. Rong,⁴ P. Wang,⁴ Y. S. Zhu,⁴
G. Eigen,⁵ I. Ofte,⁵ B. Stugu,⁵ G. S. Abrams,⁶ M. Battaglia,⁶ D. N. Brown,⁶ J. Button-Shafer,⁶ R. N. Cahn,⁶
Y. Groyzman,⁶ R. G. Jacobsen,⁶ J. A. Kadyk,⁶ L. T. Kerth,⁶ Yu. G. Kolomensky,⁶ G. Kukartsev,⁶ D. Lopes Pegna,⁶
G. Lynch,⁶ L. M. Mir,⁶ T. J. Orimoto,⁶ M. Pripstein,⁶ N. A. Roe,⁶ M. T. Ronan,^{6,*} K. Tackmann,⁶ W. A. Wenzel,⁶
P. del Amo Sanchez,⁷ M. Barrett,⁷ T. J. Harrison,⁷ A. J. Hart,⁷ C. M. Hawkes,⁷ A. T. Watson,⁷ T. Held,⁸ H. Koch,⁸
B. Lewandowski,⁸ M. Pelizaeus,⁸ T. Schroeder,⁸ M. Steinke,⁸ J. T. Boyd,⁹ J. P. Burke,⁹ W. N. Cottingham,⁹
D. Walker,⁹ D. J. Asgeirsson,¹⁰ T. Cuhadar-Donszelmann,¹⁰ B. G. Fulsom,¹⁰ C. Hearty,¹⁰ N. S. Knecht,¹⁰
T. S. Mattison,¹⁰ J. A. McKenna,¹⁰ A. Khan,¹¹ P. Kyberd,¹¹ M. Saleem,¹¹ D. J. Sherwood,¹¹ L. Teodorescu,¹¹
V. E. Blinov,¹² A. D. Bukin,¹² V. P. Druzhinin,¹² V. B. Golubev,¹² A. P. Onuchin,¹² S. I. Serednyakov,¹²
Yu. I. Skovpen,¹² E. P. Solodov,¹² K. Yu Todyshev,¹² M. Bondioli,¹³ M. Bruinsma,¹³ M. Chao,¹³ S. Curry,¹³
I. Eschrich,¹³ D. Kirkby,¹³ A. J. Lankford,¹³ P. Lund,¹³ M. Mandelkern,¹³ E. C. Martin,¹³ D. P. Stoker,¹³
S. Abachi,¹⁴ C. Buchanan,¹⁴ S. D. Foulkes,¹⁵ J. W. Gary,¹⁵ F. Liu,¹⁵ O. Long,¹⁵ B. C. Shen,¹⁵ L. Zhang,¹⁵
E. J. Hill,¹⁶ H. P. Paar,¹⁶ S. Rahatlou,¹⁶ V. Sharma,¹⁶ J. W. Berryhill,¹⁷ C. Campagnari,¹⁷ A. Cunha,¹⁷
B. Dahmes,¹⁷ T. M. Hong,¹⁷ D. Kovalskyi,¹⁷ J. D. Richman,¹⁷ T. W. Beck,¹⁸ A. M. Eisner,¹⁸ C. J. Flacco,¹⁸
C. A. Heusch,¹⁸ J. Kroseberg,¹⁸ W. S. Lockman,¹⁸ T. Schalk,¹⁸ B. A. Schumm,¹⁸ A. Seiden,¹⁸ D. C. Williams,¹⁸
M. G. Wilson,¹⁸ L. O. Winstrom,¹⁸ E. Chen,¹⁹ C. H. Cheng,¹⁹ A. Dvoretzkii,¹⁹ F. Fang,¹⁹ D. G. Hitlin,¹⁹
I. Narsky,¹⁹ T. Piatenko,¹⁹ F. C. Porter,¹⁹ G. Mancinelli,²⁰ B. T. Meadows,²⁰ K. Mishra,²⁰ M. D. Sokoloff,²⁰
F. Blanc,²¹ P. C. Bloom,²¹ S. Chen,²¹ W. T. Ford,²¹ J. F. Hirschauer,²¹ A. Kreisel,²¹ M. Nagel,²¹ U. Nauenberg,²¹
A. Olivas,²¹ J. G. Smith,²¹ K. A. Ulmer,²¹ S. R. Wagner,²¹ J. Zhang,²¹ A. Chen,²² E. A. Eckhart,²² A. Soffer,²²
W. H. Toki,²² R. J. Wilson,²² F. Winklmeier,²² Q. Zeng,²² D. D. Altenburg,²³ E. Feltresi,²³ A. Hauke,²³
H. Jasper,²³ J. Merkel,²³ A. Petzold,²³ B. Spaan,²³ K. Wacker,²³ T. Brandt,²⁴ V. Klose,²⁴ H. M. Lacker,²⁴
W. F. Mader,²⁴ R. Nogowski,²⁴ J. Schubert,²⁴ K. R. Schubert,²⁴ R. Schwierz,²⁴ J. E. Sundermann,²⁴ A. Volk,²⁴
D. Bernard,²⁵ G. R. Bonneaud,²⁵ E. Latour,²⁵ Ch. Thiebaux,²⁵ M. Verderi,²⁵ P. J. Clark,²⁶ W. Gradl,²⁶
F. Muheim,²⁶ S. Playfer,²⁶ A. I. Robertson,²⁶ Y. Xie,²⁶ M. Andreotti,²⁷ D. Bettoni,²⁷ C. Bozzi,²⁷ R. Calabrese,²⁷
G. Cibinetto,²⁷ E. Luppi,²⁷ M. Negrini,²⁷ A. Petrella,²⁷ L. Piemontese,²⁷ E. Prencipe,²⁷ F. Anulli,²⁸
R. Baldini-Ferroli,²⁸ A. Calcaterra,²⁸ R. de Sangro,²⁸ G. Finocchiaro,²⁸ S. Pacetti,²⁸ P. Patteri,²⁸ I. M. Peruzzi,^{28,†}
M. Piccolo,²⁸ M. Rama,²⁸ A. Zallo,²⁸ A. Buzzo,²⁹ R. Contri,²⁹ M. Lo Vetere,²⁹ M. M. Macri,²⁹ M. R. Monge,²⁹
S. Passaggio,²⁹ C. Patrignani,²⁹ E. Robutti,²⁹ A. Santroni,²⁹ S. Tosi,²⁹ K. S. Chaisanguanthum,³⁰ M. Morii,³⁰
J. Wu,³⁰ R. S. Dubitzky,³¹ J. Marks,³¹ S. Schenk,³¹ U. Uwer,³¹ D. J. Bard,³² P. D. Dauncey,³² R. L. Flack,³²
J. A. Nash,³² M. B. Nikolich,³² W. Panduro Vazquez,³² P. K. Behera,³³ X. Chai,³³ M. J. Charles,³³ U. Mallik,³³
N. T. Meyer,³³ V. Ziegler,³³ J. Cochran,³⁴ H. B. Crawley,³⁴ L. Dong,³⁴ V. Eyges,³⁴ W. T. Meyer,³⁴ S. Prell,³⁴
E. I. Rosenberg,³⁴ A. E. Rubin,³⁴ A. V. Gritsan,³⁵ C. K. Lae,³⁵ A. G. Denig,³⁶ M. Fritsch,³⁶ G. Schott,³⁶
N. Arnaud,³⁷ J. Béguilleux,³⁷ M. Davier,³⁷ G. Grosdidier,³⁷ A. Höcker,³⁷ V. Lepeltier,³⁷ F. Le Diberder,³⁷
A. M. Lutz,³⁷ S. Pruvot,³⁷ S. Rodier,³⁷ P. Roudeau,³⁷ M. H. Schune,³⁷ J. Serrano,³⁷ V. Sordini,³⁷ A. Stocchi,³⁷
W. F. Wang,³⁷ G. Wormser,³⁷ D. J. Lange,³⁸ D. M. Wright,³⁸ C. A. Chavez,³⁹ I. J. Forster,³⁹ J. R. Fry,³⁹
E. Gabathuler,³⁹ R. Gamet,³⁹ D. E. Hutchcroft,³⁹ D. J. Payne,³⁹ K. C. Schofield,³⁹ C. Touramanis,³⁹ A. J. Bevan,⁴⁰
K. A. George,⁴⁰ F. Di Lodovico,⁴⁰ W. Menges,⁴⁰ R. Sacco,⁴⁰ G. Cowan,⁴¹ H. U. Flaecher,⁴¹ D. A. Hopkins,⁴¹
P. S. Jackson,⁴¹ T. R. McMahon,⁴¹ F. Salvatore,⁴¹ A. C. Wren,⁴¹ D. N. Brown,⁴² C. L. Davis,⁴² J. Allison,⁴³
N. R. Barlow,⁴³ R. J. Barlow,⁴³ Y. M. Chia,⁴³ C. L. Edgar,⁴³ G. D. Lafferty,⁴³ T. J. West,⁴³ J. I. Yi,⁴³ C. Chen,⁴⁴
W. D. Hulsbergen,⁴⁴ A. Jawahery,⁴⁴ D. A. Roberts,⁴⁴ G. Simi,⁴⁴ G. Blaylock,⁴⁵ C. Dallapiccola,⁴⁵ S. S. Hertzbach,⁴⁵
X. Li,⁴⁵ T. B. Moore,⁴⁵ E. Salvati,⁴⁵ S. Saremi,⁴⁵ R. Cowan,⁴⁶ G. Sciolla,⁴⁶ S. J. Sekula,⁴⁶ M. Spitznagel,⁴⁶
F. Taylor,⁴⁶ R. K. Yamamoto,⁴⁶ H. Kim,⁴⁷ S. E. Mclachlin,⁴⁷ P. M. Patel,⁴⁷ S. H. Robertson,⁴⁷ A. Lazzaro,⁴⁸
V. Lombardo,⁴⁸ F. Palombo,⁴⁸ J. M. Bauer,⁴⁹ L. Cremaldi,⁴⁹ V. Eschenburg,⁴⁹ R. Godang,⁴⁹ R. Kroeger,⁴⁹
D. A. Sanders,⁴⁹ D. J. Summers,⁴⁹ H. W. Zhao,⁴⁹ S. Brunet,⁵⁰ D. Côté,⁵⁰ M. Simard,⁵⁰ P. Taras,⁵⁰ F. B. Viaud,⁵⁰

H. Nicholson,⁵¹ N. Cavallo,^{52, †} G. De Nardo,⁵² F. Fabozzi,^{52, †} C. Gatto,⁵² L. Lista,⁵² D. Monorchio,⁵² P. Paolucci,⁵² D. Piccolo,⁵² C. Sciacca,⁵² M. A. Baak,⁵³ G. Raven,⁵³ H. L. Snoek,⁵³ C. P. Jessop,⁵⁴ J. M. LoSecco,⁵⁴ G. Benelli,⁵⁵ L. A. Corwin,⁵⁵ K. K. Gan,⁵⁵ K. Honscheid,⁵⁵ D. Hufnagel,⁵⁵ H. Kagan,⁵⁵ R. Kass,⁵⁵ J. P. Morris,⁵⁵ A. M. Rahimi,⁵⁵ J. J. Regensburger,⁵⁵ R. Ter-Antonyan,⁵⁵ Q. K. Wong,⁵⁵ N. L. Blount,⁵⁶ J. Brau,⁵⁶ R. Frey,⁵⁶ O. Igonkina,⁵⁶ J. A. Kolb,⁵⁶ M. Lu,⁵⁶ R. Rahmat,⁵⁶ N. B. Sinev,⁵⁶ D. Strom,⁵⁶ J. Strube,⁵⁶ E. Torrence,⁵⁶ A. Gaz,⁵⁷ M. Margoni,⁵⁷ M. Morandin,⁵⁷ A. Pompili,⁵⁷ M. Posocco,⁵⁷ M. Rotondo,⁵⁷ F. Simonetto,⁵⁷ R. Stroili,⁵⁷ C. Voci,⁵⁷ E. Ben-Haim,⁵⁸ H. Briand,⁵⁸ J. Chauveau,⁵⁸ P. David,⁵⁸ L. Del Buono,⁵⁸ Ch. de la Vaissière,⁵⁸ O. Hamon,⁵⁸ B. L. Hartfiel,⁵⁸ Ph. Leruste,⁵⁸ J. Malclès,⁵⁸ J. Ocariz,⁵⁸ A. Perez,⁵⁸ J. Prendki,⁵⁸ L. Gladney,⁵⁹ M. Biasini,⁶⁰ R. Covarelli,⁶⁰ E. Manoni,⁶⁰ C. Angelini,⁶¹ G. Batignani,⁶¹ S. Bettarini,⁶¹ G. Calderini,⁶¹ M. Carpinelli,⁶¹ R. Cenci,⁶¹ F. Forti,⁶¹ M. A. Giorgi,⁶¹ A. Lusiani,⁶¹ G. Marchiori,⁶¹ M. A. Mazur,⁶¹ M. Morganti,⁶¹ N. Neri,⁶¹ E. Paoloni,⁶¹ G. Rizzo,⁶¹ J. J. Walsh,⁶¹ M. Haire,⁶² J. Biesiada,⁶³ P. Elmer,⁶³ Y. P. Lau,⁶³ C. Lu,⁶³ J. Olsen,⁶³ A. J. S. Smith,⁶³ A. V. Telnov,⁶³ E. Baracchini,⁶⁴ F. Bellini,⁶⁴ G. Cavoto,⁶⁴ A. D’Orazio,⁶⁴ D. del Re,⁶⁴ E. Di Marco,⁶⁴ R. Faccini,⁶⁴ F. Ferrarotto,⁶⁴ F. Ferroni,⁶⁴ M. Gaspero,⁶⁴ P. D. Jackson,⁶⁴ L. Li Gioi,⁶⁴ M. A. Mazzoni,⁶⁴ S. Morganti,⁶⁴ G. Piredda,⁶⁴ F. Polci,⁶⁴ F. Renga,⁶⁴ C. Voena,⁶⁴ M. Ebert,⁶⁵ H. Schröder,⁶⁵ R. Waldi,⁶⁵ T. Adye,⁶⁶ G. Castelli,⁶⁶ B. Franek,⁶⁶ E. O. Olaiya,⁶⁶ S. Ricciardi,⁶⁶ W. Roethel,⁶⁶ F. F. Wilson,⁶⁶ R. Aleksan,⁶⁷ S. Emery,⁶⁷ M. Escalier,⁶⁷ A. Gaidot,⁶⁷ S. F. Ganzhur,⁶⁷ G. Hamel de Monchenault,⁶⁷ W. Kozanecki,⁶⁷ M. Legendre,⁶⁷ G. Vasseur,⁶⁷ Ch. Yèche,⁶⁷ M. Zito,⁶⁷ X. R. Chen,⁶⁸ H. Liu,⁶⁸ W. Park,⁶⁸ M. V. Purohit,⁶⁸ J. R. Wilson,⁶⁸ M. T. Allen,⁶⁹ D. Aston,⁶⁹ R. Bartoldus,⁶⁹ P. Bechtle,⁶⁹ N. Berger,⁶⁹ R. Claus,⁶⁹ J. P. Coleman,⁶⁹ M. R. Convery,⁶⁹ J. C. Dingfelder,⁶⁹ J. Dorfan,⁶⁹ G. P. Dubois-Felsmann,⁶⁹ D. Dujmic,⁶⁹ W. Dunwoodie,⁶⁹ R. C. Field,⁶⁹ T. Glanzman,⁶⁹ S. J. Gowdy,⁶⁹ M. T. Graham,⁶⁹ P. Grenier,⁶⁹ V. Halyo,⁶⁹ C. Hast,⁶⁹ T. Hryn’ova,⁶⁹ W. R. Innes,⁶⁹ M. H. Kelsey,⁶⁹ P. Kim,⁶⁹ D. W. G. S. Leith,⁶⁹ S. Li,⁶⁹ S. Luitz,⁶⁹ V. Luth,⁶⁹ H. L. Lynch,⁶⁹ D. B. MacFarlane,⁶⁹ H. Marsiske,⁶⁹ R. Messner,⁶⁹ D. R. Muller,⁶⁹ C. P. O’Grady,⁶⁹ V. E. Ozcan,⁶⁹ A. Perazzo,⁶⁹ M. Perl,⁶⁹ T. Pulliam,⁶⁹ B. N. Ratcliff,⁶⁹ A. Roodman,⁶⁹ A. A. Salnikov,⁶⁹ R. H. Schindler,⁶⁹ J. Schwiening,⁶⁹ A. Snyder,⁶⁹ J. Stelzer,⁶⁹ D. Su,⁶⁹ M. K. Sullivan,⁶⁹ K. Suzuki,⁶⁹ S. K. Swain,⁶⁹ J. M. Thompson,⁶⁹ J. Va’vra,⁶⁹ N. van Bakel,⁶⁹ A. P. Wagner,⁶⁹ M. Weaver,⁶⁹ W. J. Wisniewski,⁶⁹ M. Wittgen,⁶⁹ D. H. Wright,⁶⁹ H. W. Wulsin,⁶⁹ A. K. Yarritu,⁶⁹ K. Yi,⁶⁹ C. C. Young,⁶⁹ P. R. Burchat,⁷⁰ A. J. Edwards,⁷⁰ S. A. Majewski,⁷⁰ B. A. Petersen,⁷⁰ L. Wilden,⁷⁰ S. Ahmed,⁷¹ M. S. Alam,⁷¹ R. Bula,⁷¹ J. A. Ernst,⁷¹ V. Jain,⁷¹ B. Pan,⁷¹ M. A. Saeed,⁷¹ F. R. Wappler,⁷¹ S. B. Zain,⁷¹ W. Bugg,⁷² M. Krishnamurthy,⁷² S. M. Spanier,⁷² R. Eckmann,⁷³ J. L. Ritchie,⁷³ C. J. Schilling,⁷³ R. F. Schwitters,⁷³ J. M. Izen,⁷⁴ X. C. Lou,⁷⁴ S. Ye,⁷⁴ F. Bianchi,⁷⁵ F. Gallo,⁷⁵ D. Gamba,⁷⁵ M. Pelliccioni,⁷⁵ M. Bomben,⁷⁶ L. Bosisio,⁷⁶ C. Cartaro,⁷⁶ F. Cossutti,⁷⁶ G. Della Ricca,⁷⁶ L. Lanceri,⁷⁶ L. Vitale,⁷⁶ V. Azzolini,⁷⁷ N. Lopez-March,⁷⁷ F. Martinez-Vidal,⁷⁷ A. Oyanguren,⁷⁷ J. Albert,⁷⁸ Sw. Banerjee,⁷⁸ B. Bhuyan,⁷⁸ K. Hamano,⁷⁸ R. Kowalewski,⁷⁸ I. M. Nugent,⁷⁸ J. M. Roney,⁷⁸ R. J. Sobie,⁷⁸ J. J. Back,⁷⁹ P. F. Harrison,⁷⁹ T. E. Latham,⁷⁹ G. B. Mohanty,⁷⁹ M. Pappagallo,^{79, §} H. R. Band,⁸⁰ X. Chen,⁸⁰ S. Dasu,⁸⁰ K. T. Flood,⁸⁰ J. J. Hollar,⁸⁰ P. E. Kutter,⁸⁰ B. Mellado,⁸⁰ Y. Pan,⁸⁰ M. Pierini,⁸⁰ R. Prepost,⁸⁰ S. L. Wu,⁸⁰ Z. Yu,⁸⁰ and H. Neal⁸¹

(The BABAR Collaboration)

¹Laboratoire de Physique des Particules, IN2P3/CNRS et Université de Savoie, F-74941 Annecy-Le-Vieux, France

²Universitat de Barcelona, Facultat de Física, Departament ECM, E-08028 Barcelona, Spain

³Università di Bari, Dipartimento di Fisica and INFN, I-70126 Bari, Italy

⁴Institute of High Energy Physics, Beijing 100039, China

⁵University of Bergen, Institute of Physics, N-5007 Bergen, Norway

⁶Lawrence Berkeley National Laboratory and University of California, Berkeley, California 94720, USA

⁷University of Birmingham, Birmingham, B15 2TT, United Kingdom

⁸Ruhr Universität Bochum, Institut für Experimentalphysik 1, D-44780 Bochum, Germany

⁹University of Bristol, Bristol BS8 1TL, United Kingdom

¹⁰University of British Columbia, Vancouver, British Columbia, Canada V6T 1Z1

¹¹Brunel University, Uxbridge, Middlesex UB8 3PH, United Kingdom

¹²Budker Institute of Nuclear Physics, Novosibirsk 630090, Russia

¹³University of California at Irvine, Irvine, California 92697, USA

¹⁴University of California at Los Angeles, Los Angeles, California 90024, USA

¹⁵University of California at Riverside, Riverside, California 92521, USA

¹⁶University of California at San Diego, La Jolla, California 92093, USA

¹⁷University of California at Santa Barbara, Santa Barbara, California 93106, USA

¹⁸University of California at Santa Cruz, Institute for Particle Physics, Santa Cruz, California 95064, USA

¹⁹California Institute of Technology, Pasadena, California 91125, USA

²⁰University of Cincinnati, Cincinnati, Ohio 45221, USA

- ²¹ University of Colorado, Boulder, Colorado 80309, USA
- ²² Colorado State University, Fort Collins, Colorado 80523, USA
- ²³ Universität Dortmund, Institut für Physik, D-44221 Dortmund, Germany
- ²⁴ Technische Universität Dresden, Institut für Kern- und Teilchenphysik, D-01062 Dresden, Germany
- ²⁵ Laboratoire Leprince-Ringuet, CNRS/IN2P3, Ecole Polytechnique, F-91128 Palaiseau, France
- ²⁶ University of Edinburgh, Edinburgh EH9 3JZ, United Kingdom
- ²⁷ Università di Ferrara, Dipartimento di Fisica and INFN, I-44100 Ferrara, Italy
- ²⁸ Laboratori Nazionali di Frascati dell'INFN, I-00044 Frascati, Italy
- ²⁹ Università di Genova, Dipartimento di Fisica and INFN, I-16146 Genova, Italy
- ³⁰ Harvard University, Cambridge, Massachusetts 02138, USA
- ³¹ Universität Heidelberg, Physikalisches Institut, Philosophenweg 12, D-69120 Heidelberg, Germany
- ³² Imperial College London, London, SW7 2AZ, United Kingdom
- ³³ University of Iowa, Iowa City, Iowa 52242, USA
- ³⁴ Iowa State University, Ames, Iowa 50011-3160, USA
- ³⁵ Johns Hopkins University, Baltimore, Maryland 21218, USA
- ³⁶ Universität Karlsruhe, Institut für Experimentelle Kernphysik, D-76021 Karlsruhe, Germany
- ³⁷ Laboratoire de l'Accélérateur Linéaire, IN2P3/CNRS et Université Paris-Sud 11, Centre Scientifique d'Orsay, B. P. 34, F-91898 ORSAY Cedex, France
- ³⁸ Lawrence Livermore National Laboratory, Livermore, California 94550, USA
- ³⁹ University of Liverpool, Liverpool L69 7ZE, United Kingdom
- ⁴⁰ Queen Mary, University of London, E1 4NS, United Kingdom
- ⁴¹ University of London, Royal Holloway and Bedford New College, Egham, Surrey TW20 0EX, United Kingdom
- ⁴² University of Louisville, Louisville, Kentucky 40292, USA
- ⁴³ University of Manchester, Manchester M13 9PL, United Kingdom
- ⁴⁴ University of Maryland, College Park, Maryland 20742, USA
- ⁴⁵ University of Massachusetts, Amherst, Massachusetts 01003, USA
- ⁴⁶ Massachusetts Institute of Technology, Laboratory for Nuclear Science, Cambridge, Massachusetts 02139, USA
- ⁴⁷ McGill University, Montréal, Québec, Canada H3A 2T8
- ⁴⁸ Università di Milano, Dipartimento di Fisica and INFN, I-20133 Milano, Italy
- ⁴⁹ University of Mississippi, University, Mississippi 38677, USA
- ⁵⁰ Université de Montréal, Physique des Particules, Montréal, Québec, Canada H3C 3J7
- ⁵¹ Mount Holyoke College, South Hadley, Massachusetts 01075, USA
- ⁵² Università di Napoli Federico II, Dipartimento di Scienze Fisiche and INFN, I-80126, Napoli, Italy
- ⁵³ NIKHEF, National Institute for Nuclear Physics and High Energy Physics, NL-1009 DB Amsterdam, The Netherlands
- ⁵⁴ University of Notre Dame, Notre Dame, Indiana 46556, USA
- ⁵⁵ Ohio State University, Columbus, Ohio 43210, USA
- ⁵⁶ University of Oregon, Eugene, Oregon 97403, USA
- ⁵⁷ Università di Padova, Dipartimento di Fisica and INFN, I-35131 Padova, Italy
- ⁵⁸ Laboratoire de Physique Nucléaire et de Hautes Energies, IN2P3/CNRS, Université Pierre et Marie Curie-Paris6, Université Denis Diderot-Paris7, F-75252 Paris, France
- ⁵⁹ University of Pennsylvania, Philadelphia, Pennsylvania 19104, USA
- ⁶⁰ Università di Perugia, Dipartimento di Fisica and INFN, I-06100 Perugia, Italy
- ⁶¹ Università di Pisa, Dipartimento di Fisica, Scuola Normale Superiore and INFN, I-56127 Pisa, Italy
- ⁶² Prairie View A&M University, Prairie View, Texas 77446, USA
- ⁶³ Princeton University, Princeton, New Jersey 08544, USA
- ⁶⁴ Università di Roma La Sapienza, Dipartimento di Fisica and INFN, I-00185 Roma, Italy
- ⁶⁵ Universität Rostock, D-18051 Rostock, Germany
- ⁶⁶ Rutherford Appleton Laboratory, Chilton, Didcot, Oxon, OX11 0QX, United Kingdom
- ⁶⁷ DSM/Dapnia, CEA/Saclay, F-91191 Gif-sur-Yvette, France
- ⁶⁸ University of South Carolina, Columbia, South Carolina 29208, USA
- ⁶⁹ Stanford Linear Accelerator Center, Stanford, California 94309, USA
- ⁷⁰ Stanford University, Stanford, California 94305-4060, USA
- ⁷¹ State University of New York, Albany, New York 12222, USA
- ⁷² University of Tennessee, Knoxville, Tennessee 37996, USA
- ⁷³ University of Texas at Austin, Austin, Texas 78712, USA
- ⁷⁴ University of Texas at Dallas, Richardson, Texas 75083, USA
- ⁷⁵ Università di Torino, Dipartimento di Fisica Sperimentale and INFN, I-10125 Torino, Italy
- ⁷⁶ Università di Trieste, Dipartimento di Fisica and INFN, I-34127 Trieste, Italy
- ⁷⁷ IFIC, Universitat de Valencia-CSIC, E-46071 Valencia, Spain
- ⁷⁸ University of Victoria, Victoria, British Columbia, Canada V8W 3P6
- ⁷⁹ Department of Physics, University of Warwick, Coventry CV4 7AL, United Kingdom
- ⁸⁰ University of Wisconsin, Madison, Wisconsin 53706, USA
- ⁸¹ Yale University, New Haven, Connecticut 06511, USA

(Dated: September 18, 2018)

We report the results of a CP violation analysis of the decay $B^\pm \rightarrow D_{\pi^+\pi^-\pi^0} K^\pm$, where $D_{\pi^+\pi^-\pi^0}$ indicates a neutral D meson detected in the final state $\pi^+\pi^-\pi^0$, excluding $K_S^0\pi^0$. The analysis makes use of 324 million $e^+e^- \rightarrow B\bar{B}$ events recorded by the *BABAR* experiment at the PEP-II e^+e^- storage ring. By analyzing the $\pi^+\pi^-\pi^0$ Dalitz plot distribution and the $B^\pm \rightarrow D_{\pi^+\pi^-\pi^0} K^\pm$ branching fraction and decay rate asymmetry, we calculate parameters related to the phase γ of the CKM unitarity triangle. We also measure the magnitudes and phases of the components of the $D^0 \rightarrow \pi^+\pi^-\pi^0$ decay amplitude.

PACS numbers: 13.25.Hw, 12.15.Hh, 11.30.Er

An important component of the program to study CP violation is the measurement of the angle $\gamma = \arg(-V_{ud}V_{ub}^*/V_{cd}V_{cb}^*)$ of the unitarity triangle related to the Cabibbo-Kobayashi-Maskawa quark mixing matrix [1]. The decays $B \rightarrow D^{(*)0}K^{(*)}$ can be used to measure γ with essentially no hadronic uncertainties, exploiting interference between $b \rightarrow u\bar{c}s$ and $b \rightarrow c\bar{u}s$ decay amplitudes [2]. In one of the measurement methods [3], γ is extracted by analyzing the D -decay Dalitz plot distribution in $B^\pm \rightarrow DK^\pm$ with multi-body D decays [4]. This method has only been used with the Cabibbo-favored decay $D \rightarrow K_S^0\pi^+\pi^-$ [5, 6], and Cabibbo-suppressed decays are expected to be similarly sensitive to γ [7]. We present here the first CP -violation study of $B^\pm \rightarrow DK^\pm$ with a multibody, Cabibbo-suppressed D decay, $D \rightarrow \pi^+\pi^-\pi^0$.

The data used in this analysis were collected with the *BABAR* detector at the PEP-II e^+e^- storage ring, running on the $\Upsilon(4S)$ resonance. Samples of simulated Monte Carlo (MC) events were analyzed with the same reconstruction and analysis procedures. These samples include an $e^+e^- \rightarrow B\bar{B}$ sample about five times larger than the data; a continuum $e^+e^- \rightarrow q\bar{q}$ sample, where q is a u , d , s , or c quark, with luminosity equivalent to the data; and a signal sample about 300 times larger than the data, with both phase space D decays and decays generated according to the amplitudes measured by CLEO [8]. The *BABAR* detector and the methods used for particle reconstruction and identification are described in Ref. [9].

The reader is referred to Ref. [10] for details of the event selection criteria. Briefly, we use event-shape variables to suppress the continuum background, and identify kaon and pion candidates using specific ionization and Cherenkov radiation. The invariant mass of D candidates must satisfy $1830 < M_D < 1895$ MeV/ c^2 . We require $5272 < m_{ES} < 5300$ MeV/ c^2 , where $m_{ES} \equiv \sqrt{E_{CM}^2/4 - |\mathbf{p}_B|^2}$, E_{CM} is the total e^+e^- center-of-mass (CM) energy, and \mathbf{p}_B is the B candidate CM momentum. Events must satisfy $-70 < \Delta E < 60$ MeV, where $\Delta E = E_B - E_{CM}/2$ and E_B is the B candidate CM energy. We exclude the decay mode $D \rightarrow K_S^0\pi^0$, which is a previously studied CP eigenstate not related to the method of Ref. [3], by rejecting candidates with $489 < M(\pi^+\pi^-) < 508$ MeV/ c^2 or for which the distance between the $\pi^+\pi^-$ vertex and the B^- candidate decay vertex is more than 1.5 cm. We reject $B^\pm \rightarrow$

$D_{\pi^+\pi^-\pi^0} K^\pm$ candidates in which the $K^\pm\pi^\mp$ invariant mass satisfies $1840 < M(K^\pm\pi^\mp) < 1890$ MeV/ c^2 , to suppress $B^- \rightarrow D_{K^-\pi^+}^0\rho^-$ decays. We require $d > 0.25$, where d [10] is a neural net variable that separates signal candidates (which peak toward $d = 1$) from those with a misreconstructed D (peaking toward $d = 0$). In events with multiple candidates, we keep the candidate whose m_{ES} value is closest to the nominal B^\pm mass [11].

For each $B^\pm \rightarrow D_{\pi^+\pi^-\pi^0} K^\pm$ candidate, we compute the neural net variable q [10]. The q distribution of $B\bar{B}$ events peaks toward $q = 1$, while that of continuum peaks at $q = 0$. For $\nu \in \{q, d\}$, we define the variables $\nu' \equiv \tanh^{-1}[(\nu - \frac{1}{2}(\nu_{max} + \nu_{min})) / \frac{1}{2}(\nu_{max} - \nu_{min})]$, where $q_{max} = d_{max} = 1$, $q_{min} = 0.1$, and $d_{min} = 0.25$ are the allowed ranges for q and d . The ν' variables can be conveniently fit with Gaussians, as described later.

As in Ref. [10], we identify in the MC samples ten event types, one signal and nine different backgrounds. We list them here with the labels used to refer to them throughout the paper. **DK_{sig}**: $B^\pm \rightarrow D_{\pi^+\pi^-\pi^0} K^\pm$ events that are correctly reconstructed; these are the only events considered to be signal. **DK_{bgd}**: $B^\pm \rightarrow D_{\pi^+\pi^-\pi^0} K^\pm$ events that are misreconstructed; namely, some of the particles used to form the final state do not originate from the $B^\pm \rightarrow D_{\pi^+\pi^-\pi^0} K^\pm$ decay. **D π _D** (**D π _{\not{D}}**): $B^- \rightarrow D^0\pi^-$, $D^0 \rightarrow \pi^+\pi^-\pi^0$ decays, where the decay $D^0 \rightarrow \pi^+\pi^-\pi^0$ is correctly reconstructed (misreconstructed). **DKX**: $B \rightarrow D^{(*)}K^{(*)-}$ events not containing the decay $D \rightarrow \pi^+\pi^-\pi^0$. **D π X**: $B \rightarrow D^{(*)}\pi^-$ and $B \rightarrow D^{(*)}\rho^-$ decays, excluding $D \rightarrow \pi^+\pi^-\pi^0$. **BBC_D** (**BBC _{\not{D}}**): all other $B\bar{B}$ events with a correctly reconstructed (misreconstructed) D candidate. **qq_D** (**qq _{\not{D}}**): continuum $e^+e^- \rightarrow q\bar{q}$ events with a correctly reconstructed (misreconstructed) D candidate.

The measurement of the CP parameters proceeds in three steps, each involving an unbinned maximum likelihood fit. In step 1, we measure the complex Dalitz plot amplitude $\alpha(s_+, s_-)$ for the decay $D^0 \rightarrow \pi^+\pi^-\pi^0$, where $s_\pm = m^2(\pi^\pm\pi^0)$ are the squared invariant masses of the $\pi^\pm\pi^0$ pairs. In step 2, we extract the numbers of B^+ and B^- signal events and background yields. We obtain the CP parameters in step 3.

We parameterize $\alpha(s_+, s_-)$ using the isobar model, $\alpha(s_+, s_-) = [a_{NR}e^{i\phi_{NR}} + \sum_r a_r e^{i\phi_r} A_r(s_+, s_-)]/N_\alpha$, where the first term represents a nonresonant contri-

bution, the sum is over all intermediate two-body resonances r , and N_α is such that $\int ds_+ ds_- |\alpha(s_+, s_-)|^2 = 1$. The amplitude for the decay chain $D^0 \rightarrow rC$, $r \rightarrow AB$ is $A_r(s_+, s_-) = F_r F_s (m_r^2 - M_{AB}^2 - im_r \Gamma_r(M_{AB}))^{-1}$, where m_r is the peak mass of the resonance [11], M_{AB}^2 is the squared invariant mass of the AB pair, F_r is a spin-dependent form factor [12], and $\Gamma_r(M_{AB})$ is the mass-dependent width for the resonance r [12]. The spin factors F_s are $F_0 = m_D^2$, $F_1 = M_{BC}^2 - M_{AC}^2 + (m_D^2 - m_C^2)(m_A^2 - m_B^2)M_{AB}^{-2}$, and $F_2 = (F_1^2 - \frac{1}{3}\mu_{CD}^2 \mu_{AB}^2) m_D^{-2}$, where $\mu_{jk}^2 \equiv M_{AB}^2 - 2m_j^2 - 2m_k^2 + (m_j^2 - m_k^2)^2 M_{jk}^{-2}$, and m_i is the mass of particle i [11].

In step 1, we determine the parameters a_{NR} , a_r , ϕ_{NR} , and ϕ_r by fitting a large sample of D^0 and \bar{D}^0 mesons, flavor-tagged through their production in the decay $D^{*+} \rightarrow D^0 \pi^+$ [13]. To select this sample, we require the CM momentum of the D^* candidate to be greater than 2770 MeV/ c , and $|M_{D^*} - M_D - 145.4 \text{ MeV}/c^2| < 0.6 \text{ MeV}/c^2$, where M_{D^*} is the invariant mass of the D^* candidate. The signal and background yields are obtained from a fit to the M_D distribution, modeling the signal as a Gaussian and the background as an exponential. The signal Gaussian peaks at $1863.7 \pm 0.4 \text{ MeV}/c^2$ and has a width of $17.4 \pm 0.8 \text{ MeV}/c^2$.

Of the D^0 candidates in the signal region $1848 < M_D < 1880 \text{ MeV}/c^2$, we obtain from the fit $N_S = 44780 \pm 250$ signal and $N_B = 830 \pm 70$ background events. To obtain the parameters of $\alpha(s_\pm, s_\mp)$, we fit these candidates with the probability distribution function (PDF) $N_S |\alpha(s_+, s_-)|^2 \epsilon(s_+, s_-) + N_B |f_B(s_+, s_-)|^2$, where the background PDF $f_B(s_+, s_-)$ is a binned distribution obtained from events in the sideband $1930 < M_D < 1990 \text{ MeV}/c^2$, and $\epsilon(s_+, s_-)$ is an efficiency function, parameterized as a two-dimensional third-order polynomial determined from MC. To within the MC-signal statistical uncertainty, $\epsilon(s_+, s_-) = \epsilon(s_-, s_+)$. The region $M_D < 1848 \text{ MeV}/c^2$, which contains $D^0 \rightarrow K^- \pi^+ \pi^0$ events that are absent from the signal region, is not used.

Table I summarizes the results of this fit, with systematic errors obtained by varying the masses and widths of the $\rho(1700)$ and σ resonances, setting $F_r = 1$, and varying $\epsilon(s_+, s_-)$ to account for uncertainties in reconstruction and particle identification. The Dalitz plot distribution of the data is shown in Fig. 1(a-c). The distribution is marked by three destructively interfering $\rho\pi$ amplitudes, suggesting an $I = 0$ -dominated final state [14].

The fit for step $i \in \{2, 3\}$ uses the PDF

$$\mathcal{P}_i^C = \sum_t \frac{N_t}{2\eta} (1 - CA_t) \mathcal{P}_{i,t}^{(C)}(\xi_i) \div \int \mathcal{P}_{i,t}^{(C)}(\xi'_i) d^n \xi'_i, \quad (1)$$

where ξ_i is the set of n_i event variables $\xi_1 = \{\Delta E, q', d'\}$, $\xi_2 = \{\Delta E, q', s_-, s_+\}$, t corresponds to one of the ten event types listed above, $N_t = N_t^+ + N_t^-$ is the number of events of type t , $A_t = (N_t^- - N_t^+)/N_t$ is their charge asymmetry, $C = \pm 1$ is the electric charge of the B can-

TABLE I: Result of the fit to the $D^{*+} \rightarrow D^0 \pi^+$ sample, showing the amplitudes ratios $R_r \equiv a_r/a_{\rho^+(770)}$, phase differences $\Delta\phi_r \equiv \phi_r - \phi_{\rho^+(770)}$, and fit fractions $f_r \equiv \int |a_r A_r(s_+, s_-)|^2 ds_- ds_+$. The first (second) errors are statistical (systematic). We take the mass (width) of the σ meson to be 400 (600) MeV/ c^2 .

| State | R_r (%) | $\Delta\phi_r$ ($^\circ$) | f_r (%) |
|----------------|--------------------------|-----------------------------|--------------------------|
| $\rho^+(770)$ | 100 | 0 | $67.8 \pm 0.0 \pm 0.6$ |
| $\rho^0(770)$ | $58.8 \pm 0.6 \pm 0.2$ | $16.2 \pm 0.6 \pm 0.4$ | $26.2 \pm 0.5 \pm 1.1$ |
| $\rho^-(770)$ | $71.4 \pm 0.8 \pm 0.3$ | $-2.0 \pm 0.6 \pm 0.6$ | $34.6 \pm 0.8 \pm 0.3$ |
| $\rho^+(1450)$ | $21 \pm 6 \pm 13$ | $-146 \pm 18 \pm 24$ | $0.11 \pm 0.07 \pm 0.12$ |
| $\rho^0(1450)$ | $33 \pm 6 \pm 4$ | $10 \pm 8 \pm 13$ | $0.30 \pm 0.11 \pm 0.07$ |
| $\rho^-(1450)$ | $82 \pm 5 \pm 4$ | $16 \pm 3 \pm 3$ | $1.79 \pm 0.22 \pm 0.12$ |
| $\rho^+(1700)$ | $225 \pm 18 \pm 14$ | $-17 \pm 2 \pm 3$ | $4.1 \pm 0.7 \pm 0.7$ |
| $\rho^0(1700)$ | $251 \pm 15 \pm 13$ | $-17 \pm 2 \pm 2$ | $5.0 \pm 0.6 \pm 1.0$ |
| $\rho^-(1700)$ | $200 \pm 11 \pm 7$ | $-50 \pm 3 \pm 3$ | $3.2 \pm 0.4 \pm 0.6$ |
| $f_0(980)$ | $1.50 \pm 0.12 \pm 0.17$ | $-59 \pm 5 \pm 4$ | $0.25 \pm 0.04 \pm 0.04$ |
| $f_0(1370)$ | $6.3 \pm 0.9 \pm 0.9$ | $156 \pm 9 \pm 6$ | $0.37 \pm 0.11 \pm 0.09$ |
| $f_0(1500)$ | $5.8 \pm 0.6 \pm 0.6$ | $12 \pm 9 \pm 4$ | $0.39 \pm 0.08 \pm 0.07$ |
| $f_0(1710)$ | $11.2 \pm 1.4 \pm 1.7$ | $51 \pm 8 \pm 7$ | $0.31 \pm 0.07 \pm 0.08$ |
| $f_2(1270)$ | $104 \pm 3 \pm 21$ | $-171 \pm 3 \pm 4$ | $1.32 \pm 0.08 \pm 0.10$ |
| $\sigma(400)$ | $6.9 \pm 0.6 \pm 1.2$ | $8 \pm 4 \pm 8$ | $0.82 \pm 0.10 \pm 0.10$ |
| Non-Res | $57 \pm 7 \pm 8$ | $-11 \pm 4 \pm 2$ | $0.84 \pm 0.21 \pm 0.12$ |

didate, and $\eta \equiv \sum_t N_t$. Using MC, we verify that the ξ_i and ξ_j ($i \neq j$) distributions are uncorrelated for each event type. Therefore, the PDFs $\mathcal{P}_{i,t}^{(C)}$ are the products

$$\begin{aligned} \mathcal{P}_{2,t}(\Delta E, q', d') &= \mathcal{E}_t(\Delta E) \mathcal{Q}_t(q') \mathcal{C}_t(d') \\ \mathcal{P}_{3,t}^C(\Delta E, q', s_+, s_-) &= \mathcal{E}_t(\Delta E) \mathcal{Q}_t(q') \mathcal{D}_t^C(s_+, s_-). \end{aligned} \quad (2)$$

The parameters of the Dalitz plot PDF $\mathcal{D}_{DK_{\text{sig}}}^C(s_+, s_-)$ are obtained from the data as described below. Those of all other functions in Eq. (2) are obtained from the MC samples. The functions $\mathcal{E}_t(\Delta E)$ are parameterized as the sum of a Gaussian and a second-order polynomial. The PDFs $\mathcal{Q}_t(q')$ and $\mathcal{C}_t(d')$ are the sum of a Gaussian and an asymmetric Gaussian. The PDF parameters are different for each event type. Assuming no CP violation in the background, we take $\mathcal{D}_t^+(s_+, s_-) = \mathcal{D}_t^-(s_-, s_+)$ and $A_t = 0$ for $t \neq DK_{\text{sig}}$. The functions $\mathcal{D}_{D\pi X}^C(s_+, s_-)$ and $\mathcal{D}_{DK_{\text{bgd}}}^C(s_+, s_-)$ are binned histograms obtained from the MC. For other event types, $\mathcal{D}_t^C(s_+, s_-) = \epsilon(s_+, s_-) \mathcal{D}_t^C(s_+, s_-)$, where the efficiency function $\epsilon(s_+, s_-)$ has different parameters for well-reconstructed and misreconstructed D candidates.

The signal Dalitz PDF accounts for interference between the $b \rightarrow u\bar{c}s$ and $b \rightarrow c\bar{u}s$ amplitudes A_u and A_c :

$$\mathcal{D}_{DK_{\text{sig}}}^\pm(s_+, s_-) = |\alpha(s_\mp, s_\pm) + z_\pm \alpha(s_\pm, s_\mp)|^2, \quad (3)$$

where $z_\pm = |A_u/A_c| e^{i(\delta \pm \gamma)}$ and δ is a CP -even phase.

In the step-2 fit, we extract the $B^\pm \rightarrow D_{\pi^+ \pi^- \pi^0} K^\pm$ signal yield and asymmetry, as well as some background yields, as described in Ref. [10]. From this fit we find $N_{DK_{\text{sig}}} = 170 \pm 29$ signal events and a decay rate asymmetry $A_{DK_{\text{sig}}} = -0.02 \pm 0.15$. Errors are statistical only.

Only the complex parameters z_{\pm} are free in the step-3 fit. This fit minimizes the function

$$\mathcal{L} = - \sum_{e=1}^{N_{\text{ev}}} \log \mathcal{P}_3^{C_e}(\xi_3^e) + \frac{1}{2} \chi^2, \quad (4)$$

where N_{ev} is the number of events in the data sample. The term $\chi^2 = \sum_{u,v=1}^2 X_u V_{uv}^{-1} X_v$ increases the sensitivity of the fit by using the results of the step-2 fit via

$$\begin{aligned} X_1 &= N_{DK_{\text{sig}}} - (n_- + n_+), \\ X_2 &= A_{DK_{\text{sig}}} - (n_- - n_+) / (n_- + n_+), \end{aligned} \quad (5)$$

where

$$n_{\pm} = N^0 \frac{\int \mathcal{D}'_{DK_{\text{sig}}}^{\pm}(s_+, s_-) ds_+ ds_-}{\int |\alpha(s_{\mp}, s_{\pm})|^2 \epsilon(s_+, s_-) ds_+ ds_-} \quad (6)$$

are the expected numbers of B^{\pm} signal events. In Eq. (6), N^0 is the product of the number $N_{B^+B^-}$ of charged B^+B^- pairs in the dataset, the branching fractions $\mathcal{B}(B^- \rightarrow D^0 K^-)$ [11] and $\mathcal{B}(D^0 \rightarrow \pi^+ \pi^- \pi^0)$ [13], and the total reconstruction efficiency $\epsilon = 11.4\%$. The error matrix V_{uv} is the sum of two components: the step-2 fit error matrix V_{uv}^{stat} , which is almost diagonal (the correlation coefficient is -2.8%), and the N^0 systematic error matrix V_{uv}^{syst} . Here $V_{12}^{\text{syst}} = V_{22}^{\text{syst}} = 0$, and $V_{11}^{\text{syst}} = \sum_{c=1}^4 (N^0 \sigma_c^{\text{rel}})^2$, where σ_c^{rel} are the relative errors on the four components $N_{B^+B^-}$ (1.1%), ϵ (3.3%), $\mathcal{B}(D \rightarrow \pi^+ \pi^- \pi^0)$ (3.8%) [13], and $\mathcal{B}(B^- \rightarrow D^0 K^-)$ (5.9%) [11].

We parameterize z_{\pm} with the polar coordinates

$$\rho_{\pm} \equiv |z_{\pm} - x_0|, \quad \theta_{\pm} \equiv \tan^{-1} \left(\frac{\Im[z_{\pm}]}{\Re[z_{\pm}] - x_0} \right), \quad (7)$$

where x_0 is a coordinate transformation parameter,

$$x_0 \equiv - \int \Re[\alpha(s_+, s_-) \alpha^*(s_-, s_+)] ds_+ ds_- = 0.850. \quad (8)$$

This parameterization is optimal due to the polar symmetry of $n_{\pm} = N^0(1 + \rho_{\pm}^2 - x_0^2)$. Other parameterizations, such as $(|A_u/A_c|, \gamma, \delta)$ or $(\Re[z_{\pm}], \Im[z_{\pm}])$, result in significant nonlinear correlations between the fit variables, which cannot be parameterized with an error matrix, and bias the fit result. The polar coordinates enable a significant improvement in sensitivity due to the χ^2 term in Eq. (4), and are determined from parameterized simulation to be unbiased. The step-3 fit yields

$$\begin{aligned} \rho_- &= 0.72 \pm 0.11 \pm 0.04, & \theta_- &= (173 \pm 42 \pm 2)^{\circ}, \\ \rho_+ &= 0.75 \pm 0.11 \pm 0.04, & \theta_+ &= (147 \pm 23 \pm 1)^{\circ}, \end{aligned} \quad (9)$$

where the first errors are statistical and the second are systematic, due only to V_{11}^{syst} . The largest correlation coefficient is $c_{\rho_- \rho_+} = 14\%$, originating from V_{11}^{syst} . All others are 1% or less. Contours of constant \mathcal{L} values are

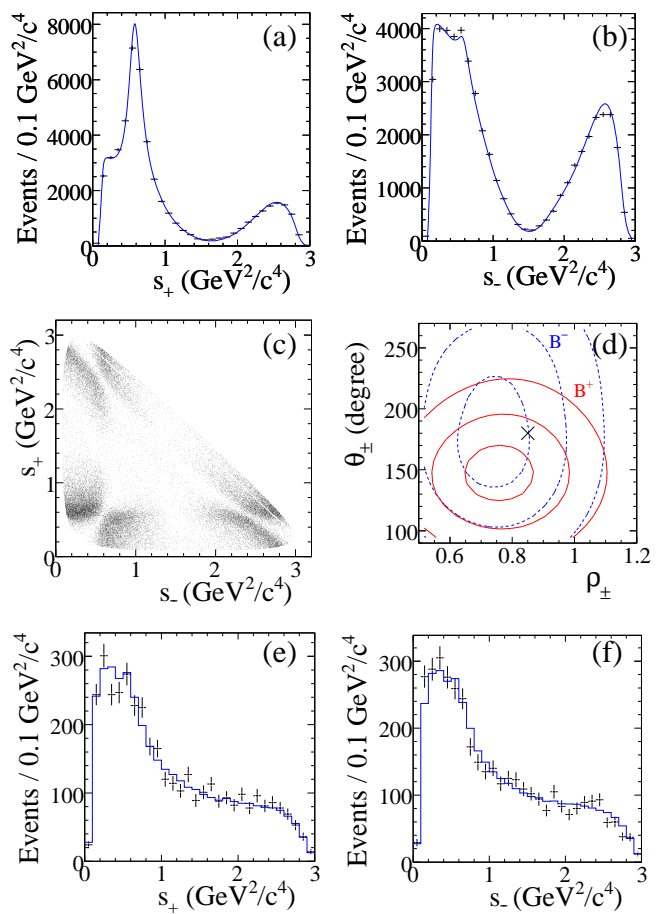


FIG. 1: (Charge conjugation is implied for all plots.) (a,b) Projections of the $D^{*+} \rightarrow D^0 \pi^+$ data events and PDF onto the Dalitz plot variables s_+ and s_- . (c) The 2-dimensional (s_+, s_-) distribution of the $D^{*+} \rightarrow D^0 \pi^+$ data. (d) One-, two-, and three-standard-deviation contours of \mathcal{L} as a function of θ_{\pm} vs. ρ_{\pm} . The solid (dashed) curves correspond to B^+ (B^-) results. The no-interference point ($\rho_{\pm} = x_0, \theta_{\pm} = 180^{\circ}$) is marked with an \times . (e,f) Projection of the $B^- \rightarrow D \pi^+ \pi^- \pi^0 K^-$ candidate data onto s_+ and s_- .

shown in Fig. 1(d). Projections of the data and the PDF onto s_+ and s_- are shown in Fig. 1(e-f).

Additional systematic errors due to the analysis procedure are evaluated for the signal branching fraction, charge asymmetry, ρ_{\pm} , and θ_{\pm} . The uncertainty in the model used for $\alpha(s_+, s_-)$ is the largest source of error on the CP parameters: $\sigma_{\rho_{\pm}}^{\text{model}} = 0.03$, $\sigma_{\theta_{\pm}}^{\text{model}} = 14^{\circ}$, $\sigma_{\theta_{\pm}}^{\text{model}} = 11^{\circ}$. This error is evaluated by removing all but the $\rho(770)$, $\rho(1450)$, $f_0(980)$, and nonresonant terms in $\alpha(s_+, s_-)$; adding an $f_2'(1525)$, an ω , and a nonresonant P-wave contribution; varying the meson “radius” parameter in F_r [12]; and propagating the errors from Table I. Uncertainties due to the masses and widths of the $\rho(1700)$ and σ resonances are small by comparison. Other errors are due to uncertainties on background yields that are

fixed in the fits [10], finite MC sample size, a possible reconstruction efficiency charge asymmetry, and uncertainties in the background PDF shapes, evaluated by comparing MC and data in signal-free sidebands of the variables M_D , ΔE , and m_{ES} . We also evaluate errors due to possible charge asymmetries in DKX and DK_{bgd} , uncertainties in particle identification and the efficiency functions, the finite s_{\pm} measurement resolution, the background PDF f_B in the D^* sample, D -flavor mistagging in the D^* sample, and correlations between the D flavor and the kaon charge in qq_D events. These errors add in quadrature to $\sigma_{\rho_{\pm}}^{\text{sys}} = 0.05$, $\sigma_{\theta_{-}}^{\text{sys}} = 19^{\circ}$, $\sigma_{\theta_{+}}^{\text{sys}} = 13^{\circ}$, and are combined with the systematic errors of Eqs. (9).

The analysis procedure is validated in several ways. Conducting the analysis on the MC sample yields results consistent with the generated values. We carry out the step-3 fit on a sample of $1800 \pm 70 B^- \rightarrow D_{\pi^+\pi^-\pi^0}^0 \pi^-$ events, obtaining the background Dalitz plot distribution from the ΔE sideband. The fit yields $\rho_- = 0.815 \pm 0.034$, $\theta_- = (186 \pm 7)^{\circ}$, $\rho_+ = 0.854 \pm 0.035$, $\theta_+ = (192 \pm 7)^{\circ}$, consistent with $\rho_{\pm} = x_0$, $\theta_{\pm} = 180^{\circ}$, which corresponds to $z_{\pm} = 0$. We verify the signal efficiency by measuring the branching fraction $\mathcal{B}(B^- \rightarrow D^0 \pi^-)$ with $D^0 \rightarrow K^- \pi^+ \pi^0$ and $D^0 \rightarrow \pi^+ \pi^- \pi^0$. We compare the fit variable distributions of data and MC events in signal-free sidebands. Good agreement is found in all cases.

In summary, using a sample of $(324.0 \pm 3.6) \times 10^6 e^+ e^- \rightarrow B\bar{B}$ events, we observe $170 \pm 29 B^{\pm} \rightarrow D_{\pi^+\pi^-\pi^0} K^{\pm}$ events. We calculate the branching fraction and decay rate asymmetry

$$\begin{aligned} \mathcal{B}(B^{\pm} \rightarrow D_{\pi^+\pi^-\pi^0} K^{\pm}) &= (4.6 \pm 0.8 \pm 0.7) \times 10^{-6}, \\ A(B^{\pm} \rightarrow D_{\pi^+\pi^-\pi^0} K^{\pm}) &= -0.02 \pm 0.15 \pm 0.03, \end{aligned} \quad (10)$$

and the CP -violation parameters

$$\begin{aligned} \rho_- &= 0.72 \pm 0.11 \pm 0.06, & \theta_- &= (173 \pm 42 \pm 19)^{\circ}, \\ \rho_+ &= 0.75 \pm 0.11 \pm 0.06, & \theta_+ &= (147 \pm 23 \pm 13)^{\circ}, \end{aligned} \quad (11)$$

where the first errors are statistical and the second are systematic. The parameters ρ_{\pm} , θ_{\pm} are defined in Eq. (7). While the errors on θ_{\pm} are too large for a meaningful determination of γ with these results alone, our errors on ρ_{\pm} are small enough to make a non-negligible contribution to the overall precision of γ in a combination of all measurements related to γ . In addition, we measure the magnitudes and phases of the components of the amplitude of the decay $D^0 \rightarrow \pi^+ \pi^- \pi^0$ in the isobar model.

We are grateful for the excellent luminosity and machine conditions provided by our PEP-II colleagues, and for the substantial dedicated effort from the computing organizations that support *BABAR*. The collaborating institutions wish to thank SLAC for its support and kind hospitality. This work is supported by DOE and NSF (USA), NSERC (Canada), IHEP (China), CEA and CNRS-IN2P3 (France), BMBF and DFG (Germany), INFN (Italy), FOM (The Netherlands), NFR (Norway), MIST (Russia), MEC (Spain), and PPARC (United Kingdom). Individuals have received support from the Marie Curie EIF (European Union) and the A. P. Sloan Foundation.

* Deceased

† Also with Università di Perugia, Dipartimento di Fisica, Perugia, Italy

‡ Also with Università della Basilicata, Potenza, Italy

§ Also with IPPP, Physics Department, Durham University, Durham DH1 3LE, United Kingdom

- [1] N. Cabibbo, Phys. Rev. Lett. **10**, 531 (1963); M. Kobayashi and T. Maskawa, Prog. Theoret. Phys. **49**, 652 (1973).
- [2] M. Gronau and D. Wyler, Phys. Lett. B **265**, 172 (1991).
- [3] A. Giri, Y. Grossman, A. Soffer and J. Zupan, Phys. Rev. D **68**, 054018 (2003); A. Bondar, Proceedings of BINP Special Analysis Meeting on Dalitz Analysis, 24-26 Sep. 2002, unpublished.
- [4] We use the symbol D to indicate any linear combination of a D^0 and a \bar{D}^0 meson state.
- [5] Belle Collaboration, A. Poluektov *et al.*, Phys. Rev. D **73**, 112009 (2006).
- [6] *BABAR* Collaboration, B. Aubert *et al.*, Phys. Rev. Lett. **95**, 121802 (2005).
- [7] Y. Grossman, Z. Ligeti and A. Soffer, Phys. Rev. D **67**, 071301 (2003).
- [8] See ‘‘Fit A’’ in CLEO Collaboration, D. Cronin-Hennessy *et al.*, Phys. Rev. D **72**, 031102 (2005).
- [9] *BABAR* Collaboration, B. Aubert *et al.*, Nucl. Instrum. Meth. A **479**, 1 (2002).
- [10] *BABAR* Collaboration, B. Aubert *et al.*, Phys. Rev. D **72**, 071102 (2005).
- [11] Particle Data Group, Y.-M. Yao *et al.*, J. Phys. G **33**, 1 (2006).
- [12] See Eq. (5) and Table I in CLEO Collaboration, S. Kopp *et al.*, Phys. Rev. D **63**, 092001 (2001).
- [13] *BABAR* Collaboration, B. Aubert *et al.*, Phys. Rev. D **74**, 091102 (2006).
- [14] C. Zemach, Phys. Rev. **133**, B1201 (1964).